Eur. Phys. J. B **40**, 243–250 (2004)
DOI: 10.1140/epjb/e2004-00266-x

THE EUROPEAN PHYSICAL JOURNAL B

Ab-initio calculation of the metal-insulator transition in sodium rings and chains and in mixed sodium-lithium systems

W. Alsheimer and B. Paulus[a]

Max-Planck-Institut für Physik komplexer Systeme, Nöthnitzer Straße 38, 01187 Dresden, Germany

Received 29 August 2003 / Received in final form 29 March 2004
Published online 31 August 2004 – © EDP Sciences, Società Italiana di Fisica, Springer-Verlag 2004

Abstract. We study how the Mott metal-insulator transition (MIT) is influenced when we deal with electrons with different angular momenta. For lithium we found an essential effect when we include p-orbitals in the description of the Hilbert space. We apply quantum-chemical methods to sodium rings and chains in order to investigate the analogue of a MIT, and how it is influenced by periodic and open boundaries. By changing the interatomic distance we analyse the character of the many-body wavefunction and the charge gap. In the second part we mimic a behaviour found in the ionic Hubbard model, where a transition from a band to a Mott insulator occurs. For that purpose we perform calculations for mixed sodium-lithium rings. In addition, we examine the question of bond alternation for the pure sodium system and the mixed sodium-lithium system, in order to determine under which conditions a Peierls distortion occurs.

PACS. 71.30.+h Metal-insulator transitions and other electronic transitions – 71.10.Fd Lattice fermion models (Hubbard model, etc.) – 31.25.Qm Electron correlation calculations for polyatomic molecules

1 Introduction

The metal-insulator transition is relatively well understood in the picture of the Hubbard model (for an overview and references see, e.g., [1]). There, the transition is driven by the ratio of the on-site Coulomb interaction U and the hopping term t. However in realistic systems it is normally insufficient to model the electronic structure with a single hopping term and an on-site Coulomb term. Furthermore the question arises how orbitals with different angular momentum quantum numbers influence the MIT. In the single-band Hubbard model only one s-type orbital per site is supplied. It was found [2] using quantum chemical ab initio methods that for lithium rings the inclusion of orbitals with p character is essential to describe quantitatively the MIT in this system. If the p orbitals are neglected, the MIT occurs at a different position in the parameter space and the energy gap in the insulating regime is much smaller. We model the ratio $\frac{U}{t}$ via the interatomic distance, where an increasing distance leads to a decreasing hopping. The on-site U stays constant. The MIT occurs in a region of interatomic distances where the many-body wavefunction changes its character rapidly from significant p contribution to purely s contribution.

In the present publication we analyse the MIT in pure sodium systems and a mixed sodium-lithium system. The latter is a ring with alternating Na and Li atoms, chosen to mimic the situation encountered in the ionic Hubbard model [3–5]. There we have, for small interatomic distances, a band insulator. When increasing the interatomic distance sufficiently a transition to a Mott insulator occurs. In addition we extend our studies from periodic boundary condition (Na rings) to open boundary conditions (Na chains). The charge gap (ionisation potential minus electron affinity) and the static electric dipole polarisability are calculated as a function of the interatomic distance. The polarisability can be used as a measure for the MIT as pointed out by Resta and Sorella [6]. Furthermore the question of a possible Peierls distortion [7] is addressed. An insulator can also be formed due to the electron-phonon coupling, where a lattice distortion yields a lower ground state energy than equidistant arrangement of the atoms.

The paper is organized as follows: In Section 2 we present some technical details and results for the Na_2 and the NaLi dimer. In Section 3 we discuss the influence of the boundary conditions in the pure Na systems and in Section 4 we examine the mixed NaLi system. Conclusions follow in Section 5.

2 Technical details

2.1 Basis sets

Mostly Gaussian type basis sets are used in quantum chemical ab initio methods to model the Hilbert space. For

[a] e-mail: beate@mpipks-dresden.mpg.de

lithium a contracted $[4s1p]$ basis was used [2], that was sufficient to describe the main feature of the system (quasi-degenerate s and p orbitals, negatively charged ions) without extreme computational costs. The selection of a proper basis set for sodium and the question of whether the use of a large-core pseudopotential is sensible for describing the core electrons is addressed in this section.

All calculations are performed with the program package MOLPRO [8–10]. Starting from a mean-field Hartree-Fock (HF) description, we reoptimise the valence wavefunction in multi-configuration self-consistent-field (MCSCF) calculations, keeping for most of the computations the $1s^2 2s^2 p^6$ core electrons frozen at the HF level, if not indicated otherwise. In this way the number of valence active-space orbitals is chosen to be equal to (or larger than) the number of Na atoms of the system, and all possible occupancies of these orbitals are accounted for. With this choice, we can properly describe the dissociation limit where each atom has one valence electron. On top of the MCSCF calculations, we apply the multi-reference averaged coupled pair functional (MRACPF) method [11,12] to deal with the dynamical correlations. Here, all configuration-state functions are included which can be generated from the MCSCF reference wavefunction by means of single and double excitations from the active orbitals.

We calculate the ionisation potential (IP), the electron affinity (EA) and the dipole polarisability of the Na atom. In all calculations the core-valence correlations are neglected. We use a 10-electron pseudopotential [13] for Na and the corresponding basis set is derived as follows. A contracted $[2s2p]$ basis is supplied with the pseudopotential [13]. An extra diffuse s-function is added (exponent 0.0094) resulting in the $[3s2p]$ basis. For the final $[3s1p]$ basis we neglect the second diffuse p function and recalculate the contraction coefficients for the remaining p function from the ^{2}P state at HF level. The IP agrees well with experiment [14] (error $\approx 3.7\%$). With our basis we obtain 88% of the experimental EA [14]. The polarisability is overestimated by about 15%, however it is known [15] that for this property the core-valence correlations are important. Although our basis is relatively small we can nevertheless describe all quantities we are interested in with sufficient accuracy.

2.2 Na_2 and NaLi dimers

For the dimers we perform MCSCF calculations with an active space of 4 orbitals (the occupation number of the corresponding natural orbitals is larger than 0.2) with the atomic closed shells kept frozen. On top of this MCSCF calculation a MRACPF calculation provides the dynamical correlation. The results for the Na_2 dimer and the NaLi dimer are listed in Table 1. With our selected basis set ecp$[3s1p]$ for Na and $[4s1p]$ for Li the dimer bond lengths are significantly too large. Both additional p functions and a d polarization function (data not in the table) reduce the dimer equilibrium distance by about 0.1 Å. Core-valence correlations, treated at the MRACPF level with the same basis as for the atom, reduce the dimer bond length further, close to the experimental value [16,17]. The static dipole polarisability is not strongly dependent on the basis set used. Additional polarization functions reduce it slightly, by about 10%, and the core-valence correlations have an influence below 3% within the basis we applied. But the core-valence correlations have a large influence on the permanent dipole moment, where they reduce the dipole moment by more than a factor of 2. When comparing with experiment, for Na_2 the polarisability is overestimated by only 12% (even for the smallest basis applied), for the NaLi dimer the best basis set applied including core-valence correlations underestimates the experimental value by 9%. The same was found by Antoine et al. [18] with CISD calculations. Although the dimer data are not fully satisfying (for better agreement with experiment we have to increase the basis set further and discuss different correlations methods) we can show that our selected basis set is sufficient to describe the main properties of the dimers and therefore of bound systems which we want to analyse in the following sections. It is not our purpose to produce very good dimer data.

Table 1. The equilibrium distance $d_{\rm dimer}$ in Å,the static dipole polarisability per molecule perpendicular to the bond α_{xx} and in bond direction α_{zz} in a.u. and the permanent dipole moment μ in a.u. are listed for Na_2 and a NaLi dimer. The static dipole polarisability and permanent dipole moment are calculated at the experimental dimer distance. The values are determined for different basis sets and compared with experiment and literature.

	basis	$d_{\rm dimer}$	α_{xx}	α_{zz}	μ
Na_2	ecp$[3s1p]$	3.392	219.5	469.5	
	ecp$[3s2p]$	3.310	211.6	449.2	
	exp [16]	3.08	$\alpha_{\rm mol} = 270$		
	CISD$(22e)$ [18]	3.09	207.8	360.4	
NaLi	ecp$[3s1p]$,$[4s1p]$	3.106	180.3	387.0	0.649
	ecp$[3s2p]$,$[4s2p]$	3.036	181.1	395.1	0.565
	exp [17]	2.89	$\alpha_{\rm mol} = 263$		0.193
	CISD$(14e)$ [18]	2.90	189.0	325.6	0.189

3 The MIT in the pure Na system with different boundary conditions

3.1 Na_{10} ring and Na_{10} chain at the equilibrium distance

To compare open and periodic boundary conditions we have selected the equidistant Na_{10} chain and the equidistant Na_{10} ring. As reference interatomic distance a_0 we have chosen the Na-Na distance from the 3-dimensional crystal (3.659 Å) [19]. We calculate the equilibrium interatomic distance and the cohesive energy per atom with different quantum chemical methods. At the closed shell Hartree-Fock (HF) level, both the ring and the chain are

not bound, the cohesive energy is positive. The equilibrium lattice constant at the HF level is about 5% smaller than a_0. A density-functional treatment with a LDA functional [20] yields the same lattice constant as HF, but the systems are bound. The LDA method works quite well for the equilibrium ground-state properties, but cannot describe the dissociation limit in the systems. For that purpose a multi-reference treatment is necessary with at least as many active orbitals as there are atoms in the system. We perform a MCSCF calculation with 11 active orbitals both for the Na_{10} ring and chain. On top of it a MRACPF calculation with single and double excitations using the same active space is applied. The equilibrium distance does not change much. The cohesive energy for the ring is 2/3 due to static correlations (MCSCF) and 1/3 due to dynamical correlations (MRACPF), whereas for the chain the dynamical correlation provides more than half of the cohesive energy. Comparing the MRACPF cohesive energy with the LDA one, we notice that LDA slightly overbinds the system. Increasing the basis set should bring the MRACPF and LDA values closer to each other.

When comparing the ring and the chain, we notice that both have nearly the same lattice constant, but the binding in the chain is about 20% weaker. The cohesive energy of the Na_2 dimer with the same basis set is 0.0077 a.u. per atom and therefore 23% weaker than the chain and 35% weaker than the ring. Both can be regarded as a system of 5 dimers. Overall, the ring and the chain system have quite similar equilibrium ground-state properties. The boundary conditions have nearly no influence when the atoms remain equidistant.

3.2 The characteristic features of the ground-state wavefunction

We want to investigate how the character of the many-body ground-state wavefunction changes when enlarging the interatomic distance from $a = 0.9a_0$ to $a = 2.0a_0$. For that purpose we perform a MCSCF calculation [21,22] for the lowest singlet state, on top of a closed-shell HF calculation. The selection of the active space is crucial: For the Na_{10} ring we found (as for the Li system) that not all important orbitals for the equilibrium distance and the dissociation limit (10 important orbitals) fall into the same irreducible representation. One of the important orbitals at the equilibrium distance falls into a different representation than the 10 orbitals of the dissociated limit. Therefore, we select as common active space the union of 11 orbitals. These orbitals were reoptimised at the MCSCF level. Finally, we performed a MRACPF calculation [11,12] on top of the MCSCF, in order to include dynamical correlation effects as completely as possible.

For the Na_{10} chain we found that the 10 important orbitals of the dissociated state are in the same irreducible representations as the 10 important orbitals at the equilibrium distance. This is different to the ring system with periodic boundary conditions. Therefore we perform here a MCSCF calculation with 10 active orbitals and proceed with a MRACPF calculation as for the ring. For the

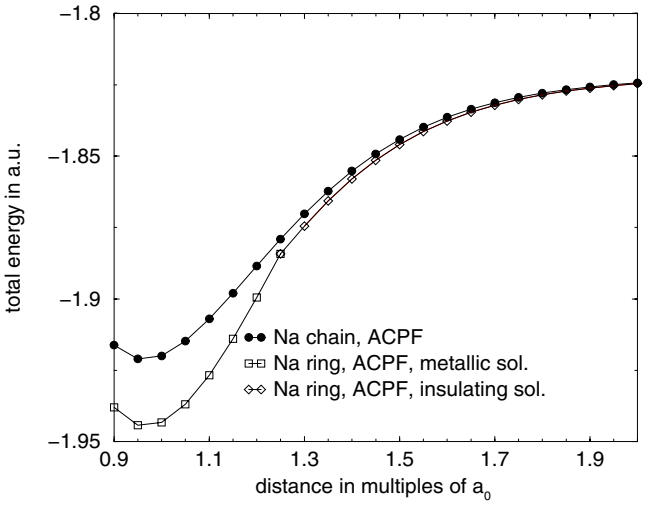

Fig. 1. MRACPF energies of the Na_{10} ring and the Na_{10} chain versus the Na-Na distance. The curves labelled "insulating solution" and "metallic solution" refer to different MCSCF zeroth-order wavefunctions used as reference for the subsequent MRACPF, cf. text.

Na_{10} chain it is interesting to look at the net charge and the p contribution of the charge population for the single atoms. Near the equilibrium lattice constant the p population is high ($\approx$0.25) and quite constant for the 6 inner atoms, and drops off for atoms belonging to the chain end. Concerning the charge transfer to the open boundaries, only the two inner atoms are almost neutral, whereas at the boundary some oscillations smaller than $0.05e$ occur. For an interatomic distance near the dissociation limit, the oscillations in the net charge disappear, all atoms are neutral. The p population is constant and quite small ($\leq$0.04) for all atoms.

Analyzing the ground state energy for the Na ring we found as for the Li ring a kink in the total energy curve. Although we included in the active space all orbitals which are important in the limits of small and large atomic distances, the total energy as a function of the Na-Na distance is still not a smooth curve (Fig. 1), because the nature of the active orbitals changes along the curve. There is a curious hysteresis-like behaviour, namely when starting the calculations from large a (wavefunction for the insulating state) and always using the previous solution as a starting point for the next smaller lattice constant, this yields a slightly different solution in the region of the MIT than when starting from the metallic regime and increasing a. For the linear Na_{10} chain we found a smooth curve, which coincides with the ring for large interatomic distances, but is higher in energy for the equilibrium distance. To analyse the kink in the ring system in more detail, we perform a Mulliken population analysis for the p orbitals (Fig. 2) of the MRACPF wavefunction as well as of the underlying MCSCF wavefunction as a function of a. Whereas for the chain the p population increases smoothly from the dissociation limit, in the ring system we found a jump to significantly higher populations at $1.25a_0$ at the

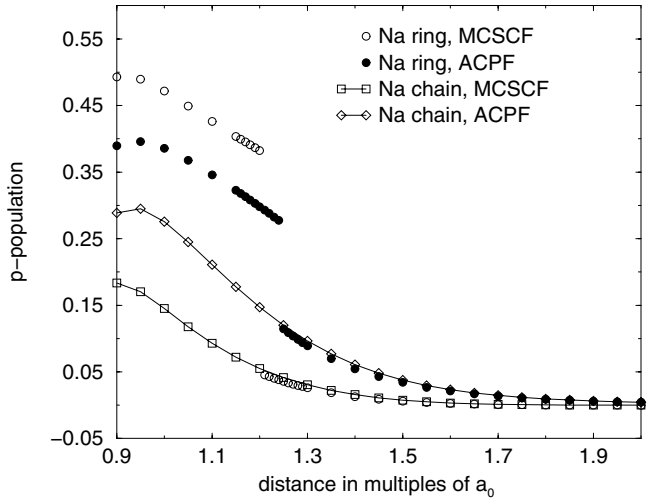

Fig. 2. The p occupation of the Na atom in a Na_{10} ring and of the inner Na atom in a Na_{10} chain versus the Na-Na distance. The p occupations are calculated using the Mulliken population analysis.

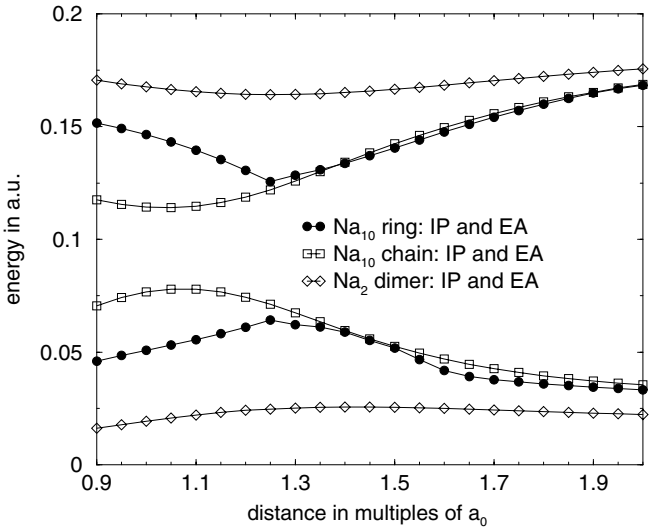

Fig. 3. MRACPF values for the EA and IP of the Na_{10} ring, the Na_{10} chain and the Na_2 dimer versus the Na-Na distance.

MRACPF level and at $1.21a_0$ at the MCSCF level. If we would characterize the metallicity by using the p population analysis, we should pin the MIT in the region where the jump of the p population occurs. But that would mean that the chain system has no metallic character and only the periodic boundary conditions force the system to be metallic. Therefore we look in the following section at the one-particle energy gap and compare for this quantity the ring and the chain system.

3.3 The one-particle energy gap

The energy gap is determined by the energy difference between the ground state of the neutral system and the ground state of the systems with one electron added and one subtracted. We calculate the MRACPF ground-state energies of the Na_n^-, Na_n and Na_n^+ systems and determine EA=E(Na_n)-E(Na_n^-) and IP=E(Na_n^+)-E(Na_n), and from IP-EA the corresponding gap. For a true metallic solid adding and removing an electron costs an energy given by the chemical potential. In finite systems, there always remains the difference between the one-particle energies of the additional and the missing electron as well as the influence of relaxation and correlation effects.

For the Li_n rings a finite-size analysis was performed [2]. The gap energy monotonously decreases with increasing number of atoms in the ring; a linear decrease is found up to $n = 12$, the largest system that is possible to treat with MRACPF. For all investigated rings ($n = 2, 6, 8, 10, 12$) we found similar behaviour with increasing distance independent of the number of atoms in the ring. In spite of this we reemphasize that, although we have a finite system instead of a real metallic system, we still see a transition from a metallic-like regime (where the gap is closing with increasing Li-Li distance) to an insulating regime where the gap is opening towards the atomic limit.

The EA and IP for the Na_{10} ring and chain, and for comparison also for the Na_2 dimer, are plotted in Figure 3. For the dissociation limit where HF fails to describe correctly the dissociation, the MRACPF calculation yields the correct atomic IP and EA for all systems evaluated. The differences occur when decreasing the interatomic distance. For the Na_2 dimer the gap is closing very slowly and below a region of $1.4a_0$ it opens again slightly. For the Na_{10} chain the gap is also closing smoothly, but much faster than for the dimer. There the minimal gap occurs at about $1.05a_0$. In the insulating regime the ring and the chain system behave very similarly, but when decreasing the interatomic distance the closing of the gap ends suddenly for the ring at that point, where the character of the wavefunction changes. Starting from there, the gap opens again and behaves like a free electron system in a box when decreasing the box length. This opening of the gap would not be so pronounced if we could perform computations in a ring with more than 10 atoms.

The behaviour in the insulating regime is independent of boundary conditions. At the equilibrium distance (around a_0) the gap for the chain is smaller by a factor of 2 than in the ring system. It is not easy to define a point for the linear system, where the MIT occurs, but taking the minimal gap as an indicator for the MIT transition, the metallic like behaviour develops for the chain at much smaller distances than for the ring. Overall the boundary conditions do not change the qualitative picture, but have a large influence on the quantitative one.

3.4 Lattice distortion

In this section we still study the pure Na system, but we allow for a bond alternation along the ring and the chain, so that the Na atoms can dimerise. For average lattice

constants larger than that where the metal-insulator transition occurs (i.e., for lattice constants where the insulating solution is the ground state) the formation of dimers is energetically favored, both for the ring and the chain system. The energy gain is due to bond formation between two Na atoms. For the ring in the metallic regime ($a \leq a_{\mathrm{MIT}}$) a Peierls distortion [7] occurs, stabilizing the dimerised state. However, decreasing the lattice constant further, we find a point ($a = 1.1a_0$ for Na_{10} ring) below which the equidistant arrangement is the ground state, which would imply a metallic state for the infinite chain. This finding is analogous to the one reported for the Li rings [2].

For the chain system we have a different result. There a dimerisation occurs for all mean Na-Na distances. Even for a mean distance smaller than the distance of the free Na-Na dimer with the same basis set ($0.9a_0$), the systems show a slight bond alternation. This is due to the open boundary conditions, which favor bond alternation. In comparison to the periodic boundary conditions, where an equidistant arrangement is favored for the equilibrium interatomic distance, the system with open boundaries always shows dimerisation. Here the boundary conditions even have a qualitative effect on the system, and only for infinite linear chains would the results coincide with the ones of periodic boundary conditions.

4 Mixed NaLi ring – a realization of the ionic Hubbard model

4.1 Hartree-Fock band structure

As a first step we study the HF band structure of the one-dimensional infinite NaLi system and compare with that of the pure Li and Na system. Using the Crystal program [23] we perform HF calculations for one-dimensional infinite chains. As a basis set in Crystal we select for Li the optimized [4s3p1d] basis set of the three-dimensional metal [24]. For Na we choose the [4s3p] basis from Dovesi et al. [25] and add a diffuse sp-function with exponent 0.08 and a d-function with exponent 0.4. In Figure 4 the Hartree-Fock (HF) band structure is shown for the optimized interatomic Li-Na distance of 5.954 a.u. In addition we plotted the back-folded Li and Na band-structure at the same interatomic distances. The Fermi energy is always shifted for all systems to zero. The main difference between NaLi and pure Na or Li occurs at the edge of the Brillouin zone, where the pure Na or Li system has no gap, whereas the mixed NaLi system has a gap of about 0.12 a.u. This clearly shows that NaLi is a band insulator, whereas Li and Na are metals at the HF level. The s and p mixing around the center of the Brillouin zone is about the same for all systems. The population analysis in the mixed system yield 3.41e for Li and 10.59e for Na, i.e. nearly half an electron moves from the Na atom to the Li atom. At the HF level the equidistant arrangement of the Li and Na atoms is stable, no dimerisation occurs in contrast to the pure Na or Li systems, whereas at the HF level we found a Peierls distortion.

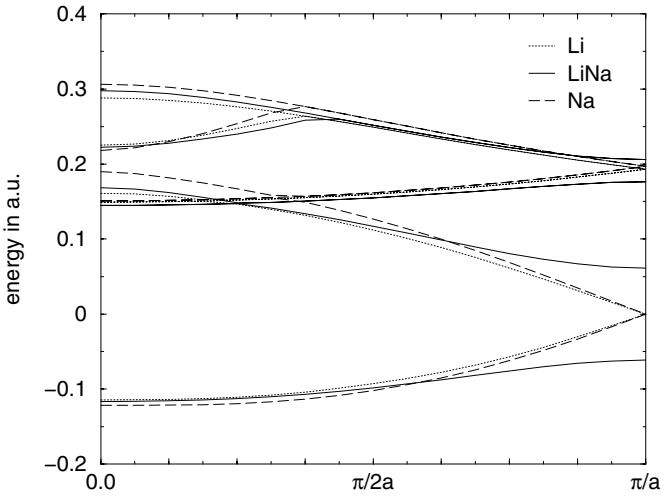

Fig. 4. Hartree-Fock band structure for the infinite NaLi chain and for the Li and Na chain back-folded to the NaLi Brillouin zone. All systems calculated at the same lattice constant (interatomic distance = 5.954 a.u.). The Fermi energy is set to zero.

An enlargement of the interatomic distance would not change the HF band structure significantly. The s and p mixing will be reduced, but the LiNa system will remain a band insulator, as Li and Na remain metallic. For an interatomic distance equal to twice the equilibrium distance the charge transfer from Na to Li is still 0.39e, which is counterintuitive. One would expect instead neutral atoms for such a large separation.

4.2 Character of the many-body wavefunction

To describe the dissociation limit in the mixed system, i.e. the transition from a band insulator to the Mott insulator, a many-body treatment is necessary. We select as a finite system an equidistant Na_5Li_5 ring with $a_0 = 5.954$ a.u. As for the Na_{10} ring we perform a MCSCF calculation with 11 active orbitals, and on top of it a MRACPF calculation. Analyzing the ground state energy for Na_5Li_5, we found as for pure Li or Na rings a kink in the MRACPF total energy curve for the Na_5Li_5 ring. Also here the quasi-degenerate s and p orbitals yield a change in the character of the wavefunction. This is shown in more detail in the p-occupation of the individual atoms (Fig. 5). The p population of the Na and Li atom is high (greater than 0.2e) up to an interatomic distance of about $1.5a_0$. It then jumps suddenly to a value smaller than 0.1e. For the equilibrium interatomic distance ($1.05a_0$ for Na_5Li_5 ring at MRACPF level) the p population is about 0.4 for both Li and Na atoms. As at the HF level, we found a charge transfer from Na to Li. At a_0 the correlation treatment reduces the charge transfer by a factor of 2 compared to HF. Whereas at the HF level the charge transfer remains nearly constant for all interatomic distances, the charge transfer at the MRACPF level drops rapidly with increasing atomic distance, has a local minimum at about $1.2a_0$ and then falls suddenly

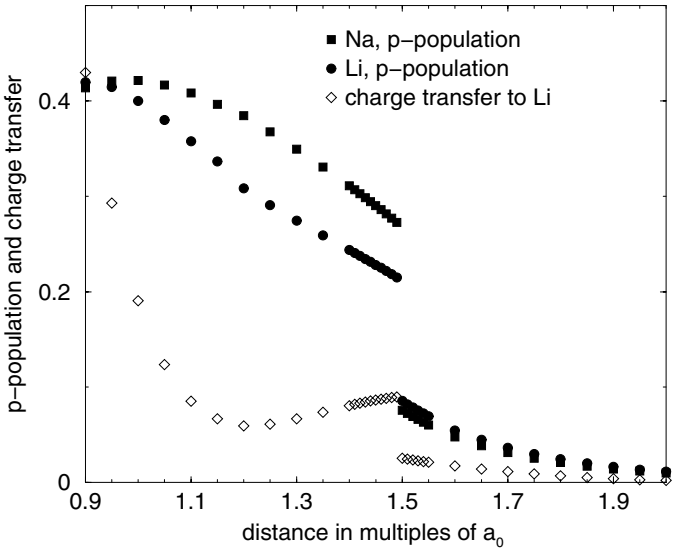

Fig. 5. The p occupation of the Na atom and the Li atom in a Na_5Li_5 ring versus the Li-Na distance. In addition the charge transfer from the Na atom to the Li atom is plotted. The p occupations and the charge transfer are calculated with the Mulliken population analysis with the MRACPF wavefunction.

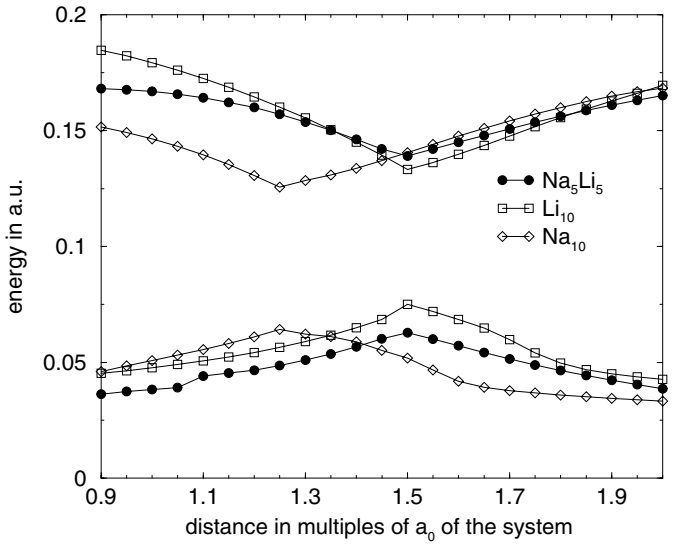

Fig. 6. MRACPF values for the EA and IP of the Na_5Li_5 ring, Na_{10} and Li_{10} ring versus the interatomic distance. The scaling of the horizontal axis always refers to the a_0 of the individual system.

when the character of the wavefunction changes. For well separated atoms we reach the expected neutral atom limit.

In summary, we can characterize the region of the band insulator as the region where we have significant p-contribution in the many-body wavefunction, and the region of the Mott insulator, where there is nearly no charge transfer and the p-contribution in the wavefunctions is negligible.

4.3 One-particle energy gap

As for the pure Na ring, we calculate the energy gap of the Na_5Li_5 ring at the MRACPF level due to adding and subtracting one electron to the system. The IP and the EA of the Na_5Li_5 ring are plotted in Figure 6. For comparison the pure Na and Li data are shown, too. In the Na_5Li_5 ring the minimal gap occurs at about $1.5a_0^{\mathrm{NaLi}}$, as it does for the pure Li system whereas for Na the minimal gap is at much smaller relative interatomic distances. The mixed system is dominated by the features of the pure Li system as there is a charge transfer from the Na to the Li atoms. For the Mott insulator (larger interatomic distance than that, where the minimal gap occurs) the pure and mixed system behave in the same manner, namely the IP and EA converge to the non-interacting atom limit. For the equilibrium distance the EA is almost the same for all three systems, whereas the IP is the largest for Li and the smallest for Na. Comparing the NaLi with the Li system the difference of the minimal gap to the gap at the equilibrium distance is not so pronounced. Only for the "metallic" systems such as Li and Na is the closing of the gap faster than in the band insulator NaLi. In other words, the electrons in the pure systems behave more like free electrons than those in NaLi and feel stronger the effects of the finite system than those in NaLi. This difference is expected to be more pronounced when the rings get longer.

4.4 Dipole polarisability

As a third quantity which can be used to indicate the MIT, we calculate the static electric dipole polarisability of the system. For a metallic system the polarisability should be infinite, therefore a steep increase of the polarisability can indicate an insulator-metal transition. The increase of the polarization approaching the MIT from the insulating side was also found in the Hubbard model [26] named dielectric catastrophe.

The static electric dipole polarisability of the NaLi system is calculated by applying a static electric field of strength up to 0.003 a.u. for the ring in the ring plane. We perform a quadratic fit with linear term for the energy of the system, $E(\mathcal{E}) = E(0) + \mu\mathcal{E} - \frac{1}{2}\alpha\mathcal{E}^2$, yielding the polarisability α and the permanent dipole moment μ. In Figure 7 we plot the polarisability per atom for the Na_5Li_5 and the pure Na_{10} and Li_{10} rings. The maximum of the polarisability occurs for all systems where the minimal gap occurs. The mixed system does not behave differently from the pure systems. The only difference for the mixed system is a small permanent dipole moment. For the equilibrium lattice constant it is about 0.07 a.u. and therefore only about $\frac{1}{10}$ of the dimer value with the same basis set. The permanent dipole moment vanishes slowly for larger interatomic distances.

4.5 Lattice distortion

Also for the mixed system we study the possibility of a lattice distortion in the system. For interatomic distances in

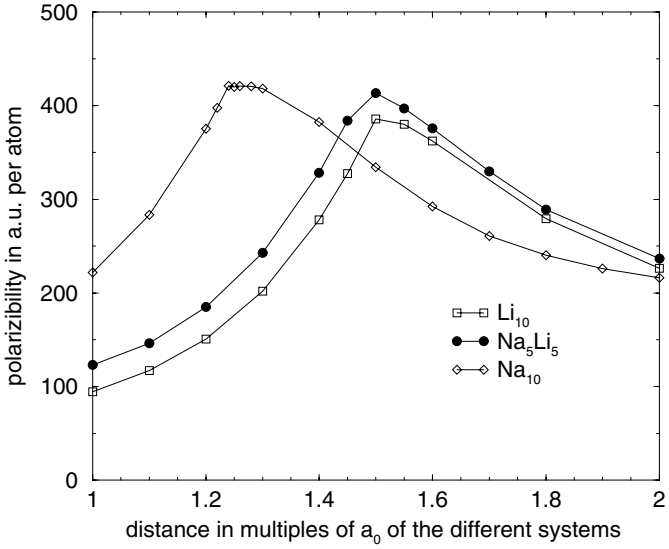

Fig. 7. The static dipole polarisability of the Na_5Li_5 ring, Na_{10} and Li_{10} ring for the electric field in the ring plane is plotted versus the interatomic distance for the MRACPF wavefunction. The scaling of the horizontal axis always refers to the a_0 of the individual system.

the Mott insulator regime the system dimerises and forms Na-Li molecules. In the region of the band insulator we found at the MRACPF level a dimerisation for a mean interatomic distance larger than $a = 1.3a_0$, below this point the equidistant arrangement of the atoms is the stable configuration. $1.3a_0$ coincides with the charge transfer minimum in the band insulator regime (see Fig. 5). This is in agreement with results obtained from the ionic Hubbard model, where in a limited region between two critical values of $\frac{U}{t}$ the bond alternation is non zero [3,5].

5 Conclusions

We have investigated the analogue of the metal-insulator transition for one-dimensional sodium and mixed lithium-sodium, applying high level quantum chemical ab initio methods. The MIT is modified from that of in the single-band Hubbard model, when we have to deal with s and p-orbitals per site. At the transition point the character of the many-body wavefunction changes from significant p to essential s character. Therefore it must be kept in mind that in a real solid the re-population of orbitals belonging to different angular momenta may have similarly strong influence on the MIT as changes in the ratio of the Hubbard U to the kinetic energy. We found that at approximately the same interatomic distance where the p character of the wavefunction changes so strongly, the one-particle energy gap is minimal.

For the pure sodium system we have analysed the influence of the boundary conditions by calculating a ring system (periodic boundaries) and a chain system (open boundaries). Whereas in the ring system during the transition the character of the wavefunction changes rapidly from significant p to pure s character, the transition in the chain system is smooth. Nevertheless a steep decrease of the p contribution is found for increasing interatomic distances. The boundary conditions have no qualitative influence on the one-particle energy gap as a function of the interatomic distance. The position however where the minimal gap occurs, and the value of the minimal gap, are strongly dependent on the boundary conditions. In the ring system a bond alternation only occurs above an interatomic distance a_{Peierls} ($a_0 \leq a_{\mathrm{Peierls}} \leq a_{\mathrm{MIT}}$) whereas the system with open boundaries dimerises for all interatomic distances.

In the second part we have evaluated the same properties for the mixed lithium-sodium system. As for pure systems, the character of the wavefunction changes from significant p contribution to pure s contribution. In addition the charge transfer from sodium to lithium is nearly zero above the transition from a band to a Mott insulator. The energy gap and the dipole polarisability are not much different from those of the pure systems. This is probably due to the fact that finite sodium or lithium rings are not real metals at the equilibrium distance, but behave more like band insulators with a small band gap. Therefore the features we observe are due to different band gaps in the systems rather than to a true qualitative change from a metal to an insulator. As in the pure systems a bond alternation is found in a region below the band to Mott insulator transition, but the dimerisation vanishes below an interatomic distance of $1.3a_0$. This is in agreement with earlier results for the ionic Hubbard model [3,5].

To analyse these properties in more detail and to approach the true metallic regime, much longer systems have to be evaluated. Unfortunately this is not possible using straightforward high-level quantum chemical methods. Some further approximations are necessary, e.g. the application of an incremental scheme as was used for neutral lithium rings [27].

The authors would like to thank Prof. Peter Fulde (Dresden), Prof. Krzysztof Rosciscewski (Krakow) and Prof. Hermann Stoll (Stuttgart) for many valuable discussions.

References

1. F. Gebhard, *The Mott Metal-Insulator Transition* (Springer, Berlin, 1997)
2. B. Paulus, K. Rosciszewski, P. Fulde, H. Stoll, Phys. Rev. B **68**, 235115 (2003)
3. M. Fabrizio, A.O. Gogolin, A.A. Nersesyan, Phys. Rev. Lett. **83**, 2014 (1999)
4. Y. Anusooya-Pati, Z.G. Soos, A. Painelli, Phys. Rev. B **63**, 205118 (2001)
5. S.R. Manmana, V. Meden, R.M. Noack, K. Schönhammer, accepted (2004)
6. R. Resta, S. Sorella, Phys. Rev. Lett. **82**, 370 (1999)
7. R.E. Peierls, *Quantum Theory of Solids* (Clarendon, London, 1955)
8. MOLPRO version 2002.6 – a package of ab initio programs written by H.-J. Werner, P.J. Knowles with contributions

from J. Almlöf, R.D. Amos, A. Bernhardsson, A. Berning, P. Celani, D.L. Cooper, M.J.O. Deegan, A.J. Dobbyn, F. Eckert, C. Hampel, G. Hetzer, T. Korona, R. Lindh, A.W. Lloyd, S.J. McNicholas, F.R. Manby, W. Meyer, M.E. Mura, A. Nicklass, P. Palmieri, R. Pitzer, G. Rauhut, M. Schütz, H. Stoll, A.J. Stone, R. Tarroni, T. Thorsteinsson
9. P.J. Knowles, H.-J. Werner, Chem. Phys. Lett. **145**, 514 (1988)
10. H.-J. Werner, P.J. Knowles, J. Chem. Phys. **89**, 5803 (1988)
11. R.J. Gdanitz, R. Ahlrichs, Chem. Phys. Lett. **143**, 413 (1988)
12. H.-J. Werner, P.J. Knowles, Theor. Chim. Acta **78**, 175 (1990)
13. P. Fuentealba, H. Preuss, H. Stoll, L.v. Szentpaly, Chem. Phys. Lett. **89**, 418 (1982)
14. A.A. Radzig, B.M. Smirnov, *Reference Data on Atoms, Molecules, and Ions* (Springer Series in Chemical Physics, edited by J.P. Toennies), Vol. 31 (Springer, Berlin, 1985)
15. W. Müller, J. Flesch, W. Meyer, J. Chem. Phys. **80**, 3297 (1983)
16. K.P. Huber, G. Herzberg, *Molecular Spectra and Molecular Structure, Constants of Diatomic Molecules* (Van Nostrand Reinhold, New York, 1979)
17. F. Engelke, G. Ennen, M. Meiwes, Chem. Phys. **66**, 391 (1982)
18. R. Antoine, D. Rayane, A.R. Allouche, M. Aubert-Frecon, E. Benichou, F.W. Dalby, Ph. Dugourd, M. Broyer, C. Guet, J. Chem. Phys. **110**, 5568 (1999)
19. C. Kittel, *Introduction to solid state physics*, 7th edn. (Wiley, New York, 1996)
20. S.J. Vosko, L. Wilk, M. Nusair, Can. J. Phys. **58**, 1200 (1980)
21. H.-J. Werner, P.J. Knowles, J. Chem. Phys. **82**, 5053 (1985)
22. P.J. Knowles, H.-J. Werner, Chem. Phys. Lett. **115**, 259 (1985)
23. V.R. Saunders, R. Dovesi, C. Roetti, M. Causa, N.M. Harrison, R. Orlando, C.M. Zicovich-Wilson, *Crystal 98 User's Manual, Theoretical Chemistry Group*, University of Torino (1998)
24. K. Doll, N.M. Harrison, V.R. Saunders, J. Phys.: Condens. Matter **11**, 5007 (1999)
25. R. Dovesi, C. Roetti, C. Freyia-Fara, M. Prencipi, Chem. Phys. **156**, 11 (1991)
26. C. Aebischer, D. Baeriswyl, R.M. Noack, Phys. Rev. Lett. **86**, 468 (2001)
27. B. Paulus, Chem. Phys. Lett. **371**, 7 (2003)